Title
COMPARATIVE ANALYSIS OF THE CELLULAR AND JOHNSON-MEHL MICROSTRUCTURES THROUGH COMPUTER SIMULATION

Author
Mahin, K.W.

Publication Date
1979-02-01

Submitted to Acta Metallurgica

LBL-8752
Preprint

COMPARATIVE ANALYSIS OF THE CELLULAR AND JOHNSON-MEHL MICROSTRUCTURES THROUGH COMPUTER SIMULATION

Kim W. Mahin, Kenton Hanson, and J. W. Morris, Jr.

February 1979

Prepared for the U. S. Department of Energy
under Contract W-7405-ENG-48

DISCLAIMER

COMPARATIVE ANALYSIS OF THE CELLULAR AND JOHNSON-MEHL MICROSTRUCTURES THROUGH COMPUTER SIMULATION

Kim W. Mahin, Kenton Hanson, and J. W. Morris, Jr.

Dept. Materials Science and Mineral Engineering, University of California, Berkeley; and Materials and Molecular Research Division, Lawrence Berkeley Laboratory, Berkeley, CA 94720

COMPARATIVE ANALYSIS OF THE CELLULAR AND JOHNSON-MEHL MICROSTRUCTURES THROUGH COMPUTER SIMULATION

Kim W. Mahin, Kenton Hanson, and J. W. Morris, Jr.

Dept. Materials Science and Mineral Engineering, University of California, Berkeley; and Materials and Molecular Research Division, Lawrence Berkeley Laboratory, Berkeley, CA 94720

Abstract

The geometric properties of polygranular microstructures of the Johnson-Mehl and cellular types have been studied through computer simulation. These prototypic microstructures arise naturally from the classical model of a phase transformation in a one-component solid through growth from a random distribution of nucleation sites. The Johnson-Mehl microstructure results in the kinetic limit of a constant nucleation rate over an essentially constant density of available nucleation sites; the cellular microstructure is produced in the kinetic limit of simultaneous activation of the available nucleation sites. Members of each of these microstructure types are similar to one another in all aspects of their geometrical statistics; they differ only through a homogeneous expansion or contraction. Their geometric features have been characterized through a combination of analytic and computer simulation studies. Comparison with available experimental results shows that the Johnson-Mehl microstructure compares well with such metallurgically diverse experimental structures as the recrystallization structure of silicon iron and the intermediate structures established during the ordering of lithium ferrite. These correspondencies suggest that

the idealized microstructures studied here may be physically relevant as well as being pedagogically useful.

completed by the impingement of growing spheres centered on these nucleation sites. This "cellular" transformation process is useful for modelling the kinetics of transformations which occur through essentially simultaneous nucleation on a volume distribution of heterogeneous nucleation sites.

The Johnson-Mehl and cellular processes have the interesting feature that, in addition to modelling the kinetics of phase transformations, they also generate characteristic product microstructures. If it is assumed that the growth of a nucleated grain ceases locally when it impinges on a second growing grain, then a cellular transformation will generate a microstructure made up of irregularly-shaped grains with planar surfaces. Each grain contains all points which are closer to its nucleus than to any other. Under the same assumption, the Johnson-Mehl process will generate a somewhat more complex aggregate of irregular grains with curved surfaces. Each grain, in this case, contains all points which are reached by linear growth from its own nucleus sooner than from any other.

Given that the "Johnson-Mehl" and "cellular" microstructures are distinct, irregular microstructures which are kinetically achievable through well-defined transformation processes, they represent potentially useful prototypes for the irregular microstructures resulting from nucleation and growth processes in real materials. Their geometric properties were studied in some detail by Meijering,[5] who obtained precise expressions or inequalities

for the mean values of several characteristic quantities, including the volume, surface area, and edge length of the average grain, as well as the average area per grain cross-section in a two-dimensional section. The statistical methods employed by Meijering[5], however, do not yield the distributions of these quantities.

From the point of view of metallurgical analysis, the distribution of geometrical features on a two-dimensional section is perhaps the most salient characteristic of a model microstructure, since these distributions may be compared directly to experimental results obtained through metallography. Moreover, physically relevant microstructural characteristics, such as the distribution of intragranular cleavage facets or slip plane sizes, may be inferred from two-dimensional distributions. However, the relevant geometric distributions are difficult to derive theoretically for irregular microstructures and are not known even for the classic cellular and Johnson-Mehl microstructures.

In the present work a computer simulation procedure was utilized to draw and analyze two-dimensional sections of three-dimensional microstructures of the Johnson-Mehl and cellular types. The distributions of important geometrical features were obtained by digital computation.

II. Computer Simulation Procedure

The computer simulation code employed in this research has been described elsewhere[6,7]. The physical process which it simulates corresponds to the transformation of a body modelled as a cube with periodic boundary conditions. The transformation is of the nucleation and growth type and, insofar as the work reported here is concerned, follows either the cellular or the Johnson-Mehl model. The microstructrure is studied through the analysis of two-dimensional sections as in conventional metallography. A two-dimensional section is constructed by the code by treating the section as a high resolution grid of points and identifying the grain to which each point belongs. The microstructural section may then be drawn and its geometric properties determined by point counting procedures which are easily and efficiently carried out in a high speed computer.

The specific manner in which the computer code assigns points within a two-dimensional section to grains of the microstructure depends on the nature of the microstructure, or on the process by which it is assumed to have been established.

In the case of the cellular microstructure, nuclei, or grain centers, are assumed to be randomly distributed with specified density throughout the parent body. A point within a two-dimensional section is an interior point of the i-th grain of the cellular microstructure if it is closer to the i-th nucleus (or to its image across the periodic boundary) than to any other grain center. A two-dimensional section at some time, t, during transformation by a cellular process may be constructed by assigning to the i-th grain those points which

are both interior to i and closer to its nucleus than the distance

$$X(t) = Gt \qquad \ldots\ldots \quad (1)$$

where G is the assumed linear growth rate. The points of the section which are assigned to no grain by this method are untransformed points of the parent matrix (Fig. 1).

In the case of the Johnson-Mehl microstructure the nuclei are assumed to appear randomly in space and time (a Poisson process[8]) to yield a constant nucleation rate per unit volume of untransformed material. The nuclei which contribute to the transformation of a cube of volume V with periodic boundary conditions by a Johnson-Mehl process having nucleation rate $\dot{N}$ per unit volume, may be identified in the following way. Ignoring the depletion of the volume available for nucleation during the transformation the probability that a nucleation event will occur somewhere in the volume V in the time interval $(\Delta t, \Delta t + dt)$ after a previous nucleation event is

$$p(\Delta t) = \dot{N}V \exp\left(-(\dot{N}V\Delta t)\right) dt. \qquad \ldots\ldots\ldots \quad (2)$$

Using this relation a random sequence of time intervals separating successive nucleation events in V is selected. The result is a succession of times, T_i, for formation of nuclei. Similarly, for each nucleus a random position $\underset{\sim}{X}_i$ in V is chosen. The nucleation sequence is then described by the set of pairs $\{\underset{\sim}{X}_i , T_i\}$. Of these hypothetical nucleation events, only those which occur in previously untransformed material are "real" in the sense that they contribute grains to the final microstructure. The condition that the i-th pair $(\underset{\sim}{X}_i, T_i)$ be real is that

$$|\underset{\sim}{X}_i - \underset{\sim}{X}_j| > G(T_i - T_j) \qquad \ldots\ldots\ldots\ldots (3)$$

for all pairs $j \neq i$. The set of "real" nucleation events, that is, the positions and times of the nuclei of grains occurring in the microstructure of a body transformed by the Johnson-Mehl process, may be identified by eliminating from the set of statistically chosen pairs $\{\underset{\sim}{X}_i, T_i\}$ those which do not satisfy the inequality (3).

Once the set of "real" nucleation events for the Johnson-Mehl microstructure has been identified, the construction of a two-dimensional section through the microstructure is straight-forward. The i-th grain in a Johnson-Mehl microstructure contains all points which are first transformed by spherical growth from the i-th nucleus. Defining

$$R_i(\underset{\sim}{X}) = |\underset{\sim}{X} - \underset{\sim}{X}_i| + GT_i, \qquad \ldots\ldots\ldots\ldots (4)$$

the point $\underset{\sim}{X}$ is in the i-th grain if

$$R_i(\underset{\sim}{X}) < R_j(\underset{\sim}{X}). \qquad (j \neq i) \qquad \ldots\ldots\ldots\ldots (5)$$

Using the inequality (5) the points of a grid covering a two-dimensional section through a Johnson-Mehl microstructure may be readily assigned to their appropriate grains.

In practice, of course, the computer code employs a grid of finite resolution to construct a picture of the microstructure. The cells of this grid are either interior points of the various grains, boundary points, in the sense that they contain a two-grain interface, or nodal cells within which three or more interfaces meet. The algorithm which analyzes the grid and assigns each cell to the appropriate grain, boundary, or node works as follows.

Let A be a cross-sectional area through the microstructure and let {i} be the set of nucleation sites. For each i, $t_i(A,i)$ is the time at which a grain growing from nucleus i will first impinge on A, and $t_f(A,i)$ is the time at which the area would be completely transformed by growth from nucleus i if no other nuclei intervened. The transformation of A is necessarily completed by the time

$$t_f(A,k) = \min \{t_f(A,i)\}. \quad \ldots\ldots\ldots\ldots \quad (6)$$

Let $G^A(\{i\})$ be the subset of {i} containing those nuclei which satisfy the relation

$$t_i(A,i) \leq t_f(A,k), \qquad i \in G^A. \quad \ldots\ldots\ldots \quad (7)$$

If G^A contains only the single element k, then all points within A are interior points of grain k. Otherwise A may be polygranular.

If G^A contains more than one element, the area A is bisected and its subareas, A', examined in turn. Since for each of the subareas $A' \subset A$ it follows that $G^{A'} \subset G^A$, only those nuclei which are members of G^A need be examined for intrusion into A'. If either of the subareas A' is polygranular, i.e., if $G^{A'}$ has multiple elements, this subarea is bisected and each of its subareas A" is examined for intrusion of the more restricted set of grains, $G^{A'}$, since $G^{A"} \subset G^{A'}$. The process is continued until either the resulting area A^n is found to be internal to a grain (G^{A^n} has only a single element) or $A^n = A_o$, the ultimate resolution of the grid. If G^{Ao} contains two elements (j and k) then the grid area is marked as an element of the boundary between j and k. If G^{Ao} contains more than two elements, then the corresponding grid section is marked as a nodal point of the microstructure, where three or more interfaces meet.

The advantage of the recursive algorithm described above is that it substantially reduces the number of areal analyses which must be made to complete a picture of the microstructure. Furthermore, the number of nuclei which must be tested for intersection at each step is reduced. The code can complete the construction of a microstructural section containing 10 - 80 grains on a 500x500 grid (250,000 point resolution grid) in only a few thousand iterative steps. The algorithm can, of course, be used in conjunction with virtually any nucleation and growth law. Its extension to three dimensions is straightforward, but is complicated by the difficulty of setting up a three-dimensional grid of reasonable resolution in a computer with finite memory. An alternate approach has been used by Hanson[9] to construct microstructures of the cellular type in three dimensions.

In a typical computer simulation experiment a 500x500 grid is used to construct two-dimensional sections through a cube having periodic boundary conditions and containing $\sim$50-300 grains. A grid of this resolution is adequate to draw the microstructural sections and analyze virtually all relevant geometric characteristics to high accuracy. Qualitative inaccuracies in microstructures generated on a 500x500 grid are uncommon, but do occasionally occur. The three most frequent "bugs" are: (1) "Fuzzy grain boundaries": the conditions specified above, that the group G^A of the area A contains more than one element, is a necessary condition for A to contain a segment of a grain boundary, but it is not a sufficient condition if A is finite. Under certain conditions the same element of the grain boundary will be claimed by adjacent elements of the grid, leading to a fuzziness

in the boundary location. (2) "Four-grain junctions": in either the Johnson-Mehl or cellular microstructure the probability that more than three grain boundary traces will intersect at a point in a two-dimensional section is identically zero. Apparent four-grain junctions are occasionally found in the computer-generated sections, due to the circumstance that the boundary segment separating two three-grain junctions is too short to be resolved. (3) "Thick boundaries": a lenticular grain lying along the boundary of two adjacent grains may be too thin to be resolved, giving rise to an apparent single grain boundary which remains thick even after all fuzziness is removed. Special subroutines (principally magnification schemes) are included in the computer code to identify these pathological cases and correct for them.

Careful construction of the two-dimensional sections allows for precise analysis of their geometrical features. Parameters such as cross-sectional area and intercept length are computed by point-counting techniques and the data tabulated in the form of geometric distributions.

III. Results and Discussion

A. Geometric similarity

A useful property of microstructures generated by the Johnson-Mehl or the cellular process is that either type of microstructure is geometrically unique to within a homogeneous expansion or contraction, i.e., a change of linear scale. In the case of the cellular microstructure geometric similarity is obvious. The microstructure is generated from randomly distributed nucleation sites with density N_V per unit volume, or one per unit volume if the unit of length is taken to be the characteristic length

$$b = (N_V)^{1/3}. \qquad \ldots\ldots\ldots\ldots (8)$$

Since the randomness of the distribution of nucleation sites is not affected by a change in the scale of length, it follows that all cellular microstructures have identical geometric statistics when referred to the characteristic length b (or to any equivalent characteristic dimension). Any histogram of any geometric property of a cellular microstructure referred to its characteristic length is valid for all microstructures generated by the cellular process.

A similar result follows in the case of the Johnson-Mehl microstructure. The Johnson-Mehl process is characterized by the expected value of the nucleation rate per unit volume, $\dot{N}$, and by the value of the linear growth rate, G. If length is measured in the characteristic unit

$$\delta_m = \dot{N}/G)^{-1/4} \qquad \ldots\ldots\ldots\ldots\ldots (9)$$

and time in the characteristic unit

$$\tau_m = (\dot{N}G^3)^{-1/4}, \qquad \ldots\ldots\ldots\ldots\ldots (10)$$

then both the nucleation and growth rates have the value one. Hence any histogram of any geometric property of a Johnson-Mehl microstructure referred to its characteristic length δ_m (or to any equivalent characteristic dimension) holds for all microstructures generated by the Johnson-Mehl process.

The volume of an average grain within a cellular microstructure is clearly

$$V_c = b^3 = (N_v)^{-1}. \quad \text{..... (11)}$$

The average grain volume in the Johnson-Mehl microstructure has been computed by Johnson and Mehl[1], by Meijering[5], and by Evans [10] to be

$$V_m = (\pi/3)^{1/4}(\Gamma(5/4))^{-1}(\delta_m)^3 = b^3. \quad \text{..... (12)}$$

Table I presents the mean values of several properties of three-dimensional crystallites in the cellular and Johnson-Mehl microstructures as computed by Meijering[5]. The properties of the Johnson-Mehl microstructure are tabulated both in units of δ_m, the characteristic length based on the nucleation and growth rates, and in units of b $(=V_m^{1/3})$, the effective grain size.

B. Morphology of Two-Dimensional Sections

Figures 1 and 2 show growth sequences leading to the cellular and Johnson-Mehl microstructures, respectively, as viewed on a two-dimensional section through a transforming cube with periodic boundary conditions. Figure 3 presents a comparison of the sections through the two microstructures.

Both growth sequences show apparent inhomogeneity in the developing microstructure. The frequent association of paired grains might, for

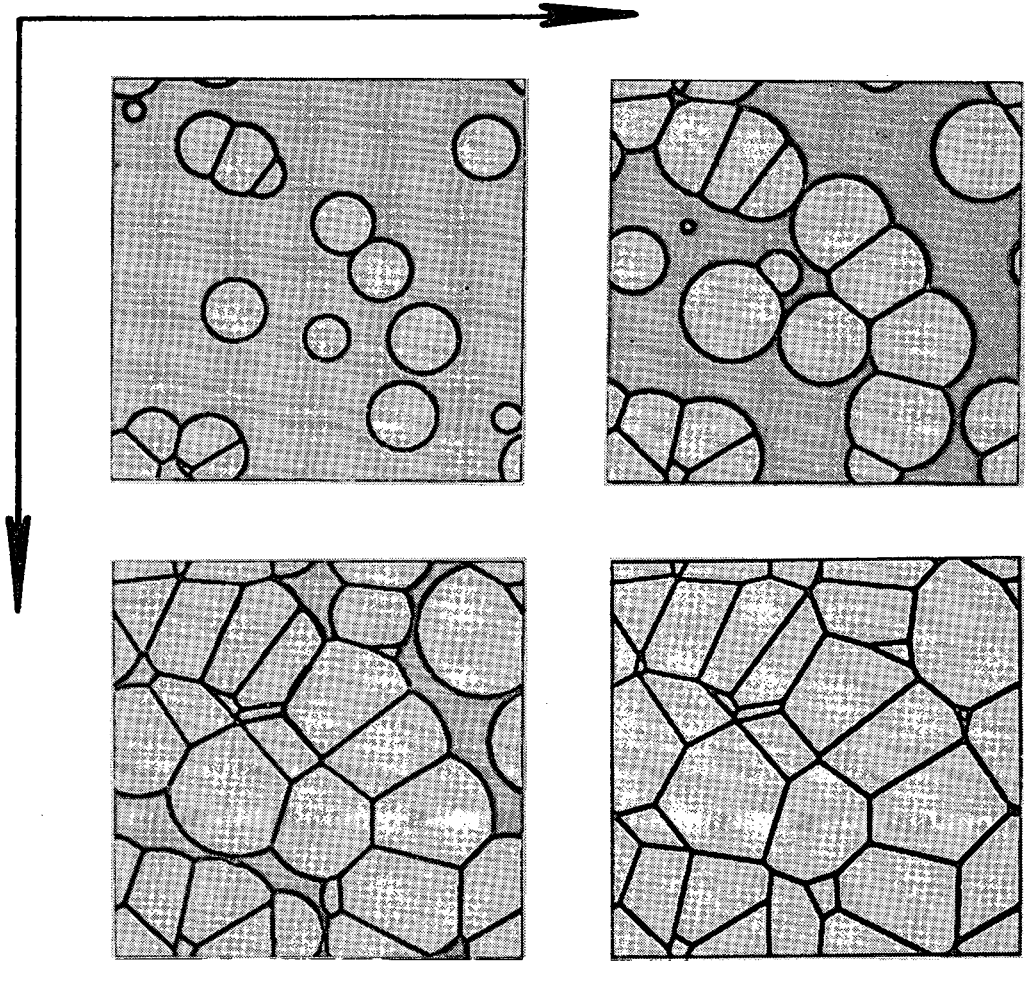

XBB 792-2551

Figure 1. Time-lapse sequence showing development of the cellular microstructure as seen on a planar section through the transforming body.

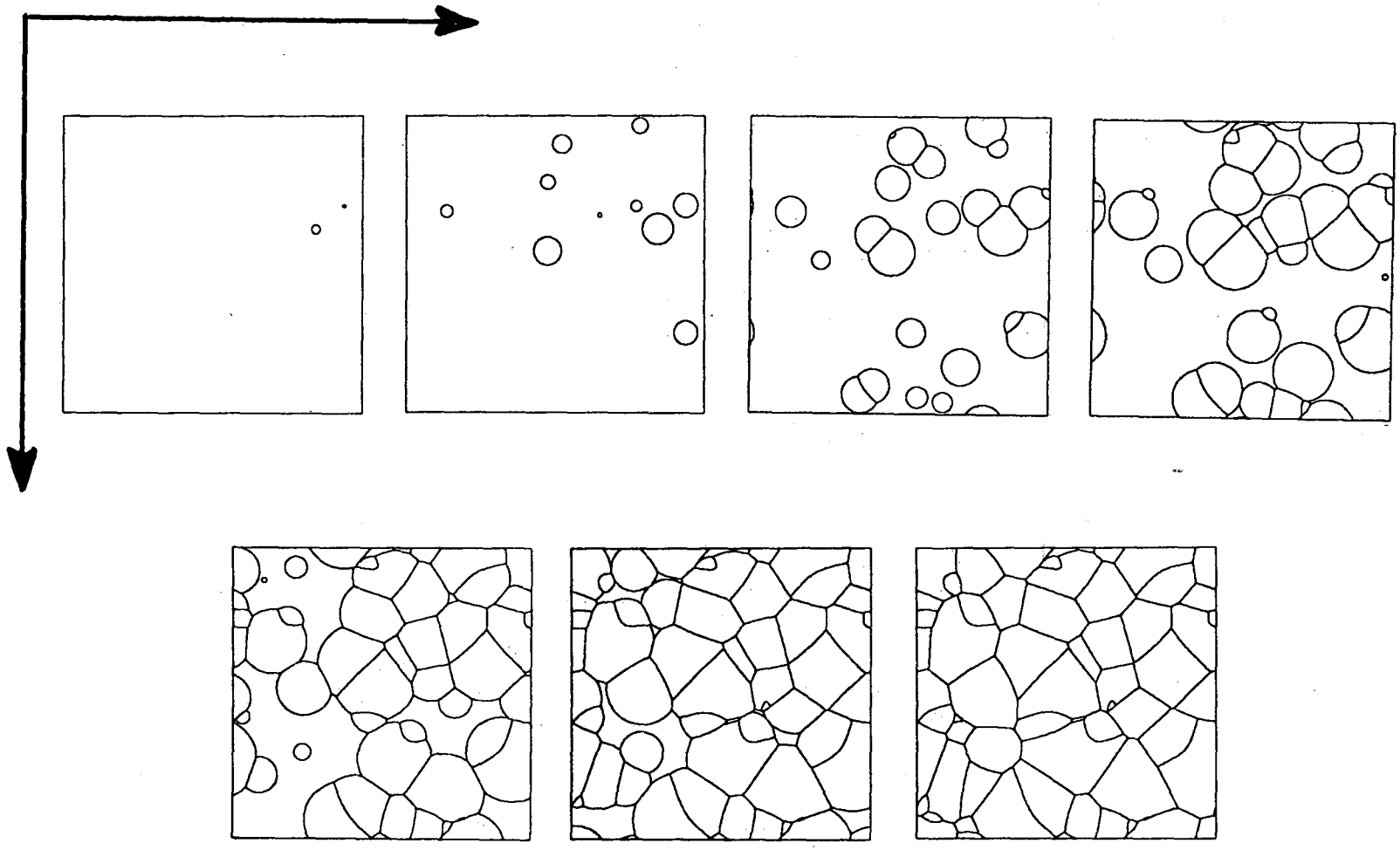

XBL 766-8042

Figure 2. Time-lapse sequence showing development of the Johnson-Mehl microstructure as seen on a planar section through the transforming body.

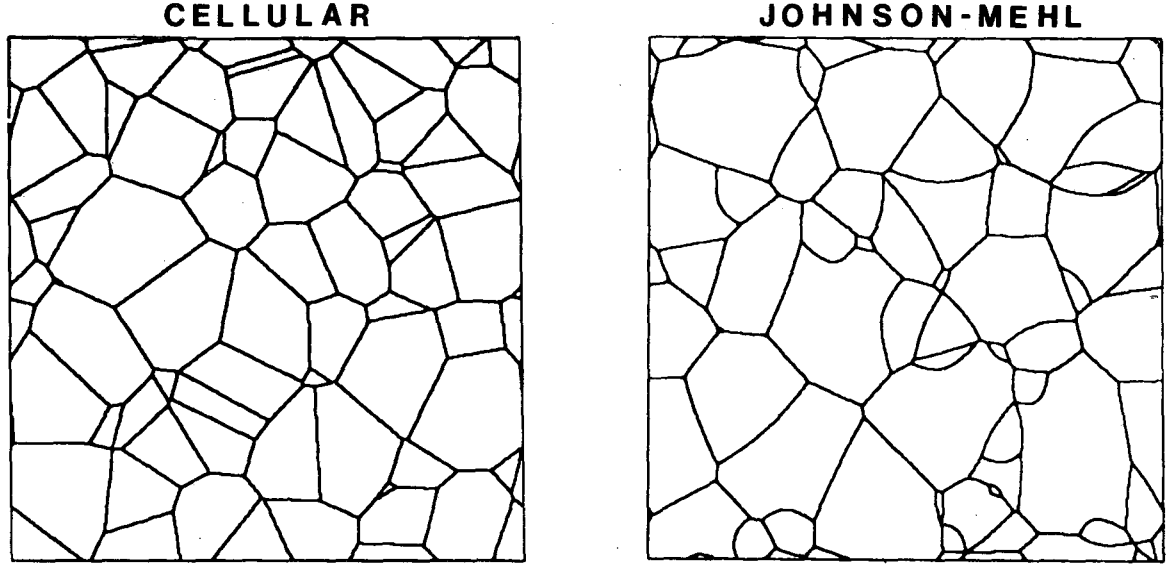

XBL 766-8054

Figure 3. Examples of sections through (a) the Cellular and (b) the Johnson-Mehl microstructure.

Table I

Mean Characteristic Quantities for a Single Grain

Quantity	Cellular	Johnson-Mehl	
Volume	b^3	b^3	$1.116(\delta_m)^3$
Surface Area	$5.821\ b^2$	$5.143\ b^2$	$5.543(\delta_m)^2$
Edge Length	17.50 b	14.71 b	$15.25\delta_m$
Number of Faces	15.54	13.28	
Number of Edges	40.61	33.84	
Number of Vertices	27.07	22.54	

example, be taken as evidence for sympathetic nucleation. Such features are, of course, straightforward results of the random nucleation process.

The cellular microstructure, Figure 1 and 3(a), is the simpler of the two types. The grains are irregular in shape, but are bounded by straight lines. All grains have three or more distinct sides.

The appearance of a two-dimensional section through the Johnson-Mehl microstructure is more complex. As shown in Figure 4, the surface of contact separating two grains which were nucleated at times t_1 and t_2, $t_1 < t_2$, is an hyperboloid of revolution. The surface is symmetric about a line joining the two nucleation sites and is convex toward the nucleus (1) which formed first. The surface obeys the equation (in polar coordinates centered on nucleus (1)):

$$r^* = [1-(r_o^*)^2] \ / \ 2[1-r_o^*\cos\theta], \qquad \ldots\ldots\ldots\ldots \quad (13)$$

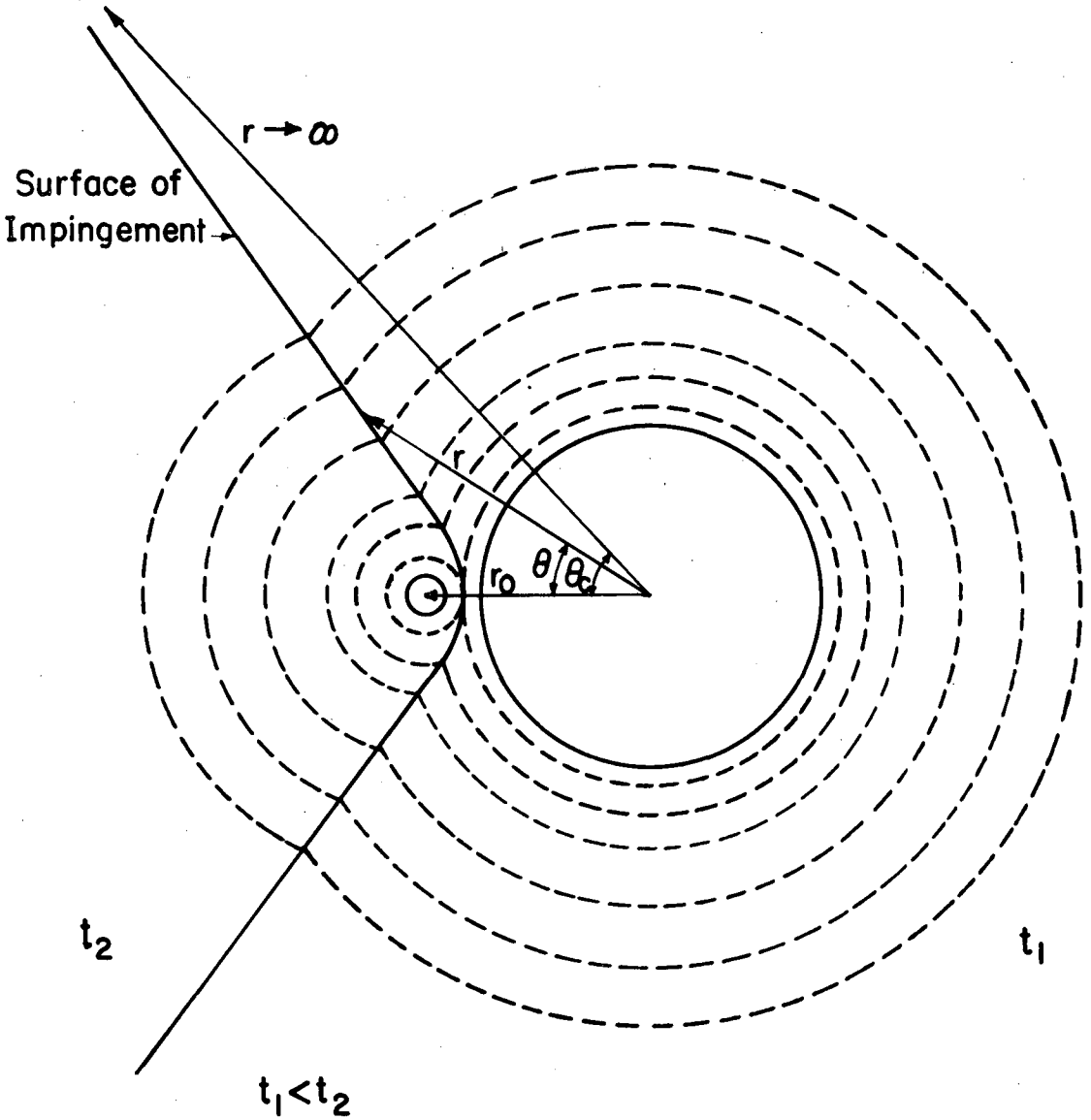

Figure 4. The surface of impingement between two grains in the Johnson-Mehl microstructure.

where

$$r^* = r/G(t_2 - t_1), \qquad \ldots\ldots\ldots\ldots \quad (14)$$

r_o is the distance separating the two nuclei and θ is the angle between the ray of length r from nucleus (1) to the surface and the reference line joining the two nuclei. As $r \to \infty$ the surface asymptotically approaches a cone of angle given by

$$\cos \theta_c = G(t_2 - t_1) \,/\, r_o. \qquad \ldots\ldots\ldots\ldots \quad (15)$$

The surface of a grain in the Johnson-Mehl microstructure is the inner envelope of the set of surfaces, described by equation (13), which separate the nucleus of the grain from each of its neighbors. These surfaces are curved, as are the lines which represent their intersections with any two dimensional plane section through the microstructure. A two-dimensional section through the Johnson-Mehl microstructure hence consists of irregular grains with curved boundaries as shown in figures 2 and 3(b).

As a consequence of the curvature of grain boundaries in the Johnson-Mehl microstructure, two-sided and one-sided grains ("caps") appear in two-dimensional sections. Examples of "caps" are shown in figures 5 and 11b. These one-sided grains occur when the two-dimensional section cuts through the nose of the hyperboloid surface separating adjacent grains.

The curvature of grain boundaries in the Johnson-Mehl microstructure has a further interesting consequence. Since the boundary between two grains is always convex toward the grain which nucleated first, it is always possible to establish the relative chronological sequence of the grains appearing in a microstructural section. Moreover, the

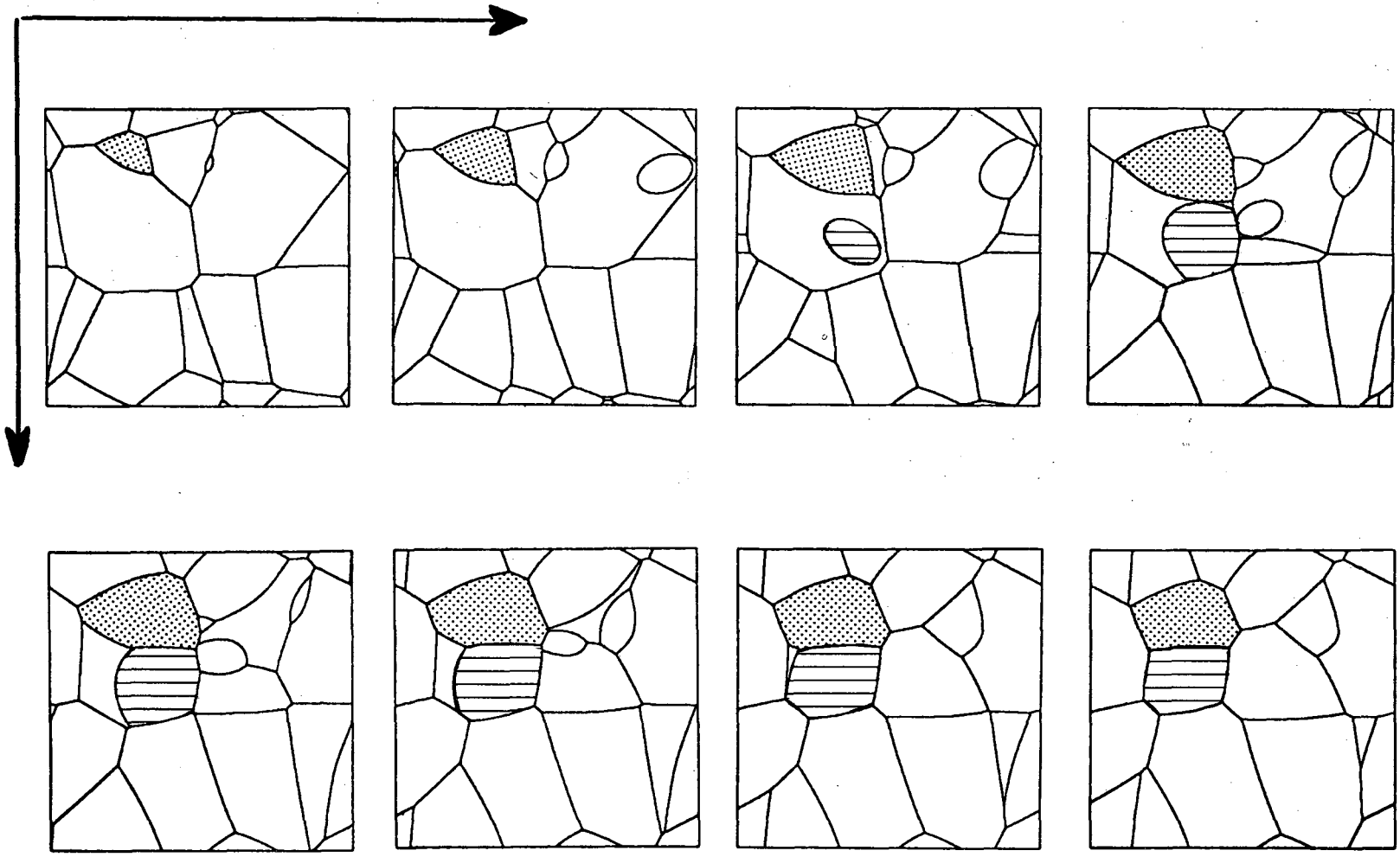

XBL 766-8052

Figure 5. A serial section through the Johnson-Mehl microstructure. The second and third frames contain grain "caps".

chemical potential differences across a boundary of non-zero surface tension is such that the boundary will always tend to migrate towards its center of curvature[11]. Thus in the initial stages of coarsening of the Johnson-Mehl microstructure a grain will always tend to grow at the expense of contiguous grains which follow it in the nucleation sequence.

C. Geometric Distributions in Two-Dimensional Microstructural Sections

The geometric properties given primary attention in this research were the number of sides per grain section, the cross-sectional area of the grain sections, and the intercept length, defined in figure 6.

(1) Number of sides per grain

In the case of the cellular microstructure, it may be easily shown that the expected number of sides per two-dimensional grain section, $\langle s \rangle$, is 6. If two-dimensional space is subdivided into cells which are simply-connected then the well-known Euler relation[11] governs the relative number of cells, (c), of cell edges, (e), and of nodal points, (p), at which cell edges intersect. In two dimensions, the relation is

$$c + p = e + 1, \qquad \text{.....} \quad (16)$$

where c = number of grain cross sections, e = number of grain boundary traces, and p = number of nodal points. This relation holds for the microstructural subdivision of any finite plane. Each nodal point in a two-dimensional section through the cellular microstructure is the intersection of three grain boundary traces, each of which is terminated by a nodal point on either end. Hence

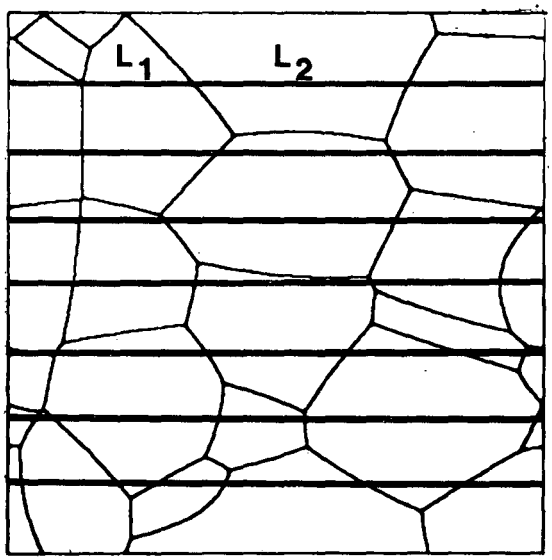

XBL 792-8447

Figure 6. A planar section of the microstructure intersected randomly by a lineal grid, yielding a number of intercept lengths, ℓ_1, ℓ_2, etc.

$$p = 2/3\ e. \qquad \ldots\ldots\ldots\ldots \quad (17)$$

Since each boundary is shared by two grain cross-sections,

$$\langle s \rangle = 2(e/c) = b \qquad \ldots\ldots\ldots\ldots \quad (18$$

in the limit of large section size.

The distribution of sidedness (i.e. of the number of grain boundary traces per grain cross-section) for two-dimensional sections through the cellular microstructure is given in figure 7. This distribution was determined by computer analysis of 5400 grain sections. Since grain sections in the cellular microstructure must have at least three sides, $\rho(s)$ is zero for $s<3$. There is, of course, no upper bound on the number of sides a grain may have, but the computer results show that grains of thirteen or more sides are very uncommon. The mean of the distribution is 6. The standard deviation is 1.68; the vast majority of the grains have between 4 and 8 sides.

The analysis of sidedness in the Johnson-Mehl microstructure is complicated by the presence of caps (figure 5). Caps are infrequent, but nonetheless real features of the Johnson-Mehl microstructure. Computer analysis has revealed the presence of caps within $\sim$0.72% of the grain sections.

Since the area of a grain section which contains a cap is not simply-connected, the Euler relation (eqn. 16) applies in a modified form. An isolated cap adds one grain section and one grain boundary trace to the microstructure, and must also be assumed to add one nodal point. The latter is arbitrarily located on the periphery of the cap but must be included to account for the unlikely but permissible case in which the cap is polygranular. If c' is the number

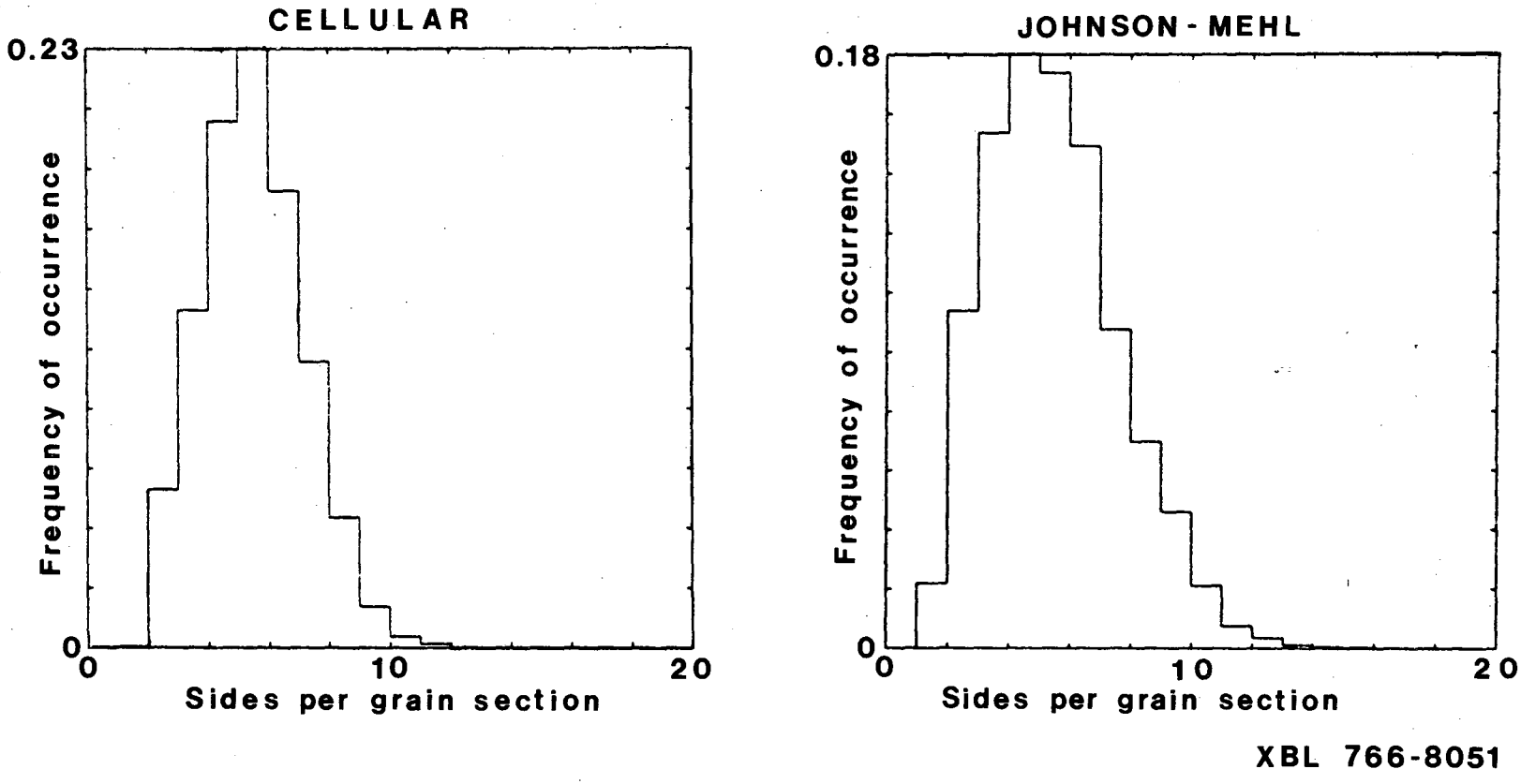

Figure 7. The distribution of the number of sides per grain for the (a) Cellular and (b) Johnson-Mehl microstructures.

of grain cross-sections which are caps, the Euler relation becomes

$$c + p = e + c' + 1. \qquad \ldots\ldots\ldots\ldots (19)$$

In this case,

$$p = 2/3(e - c') + c' \qquad \ldots\ldots\ldots\ldots (20)$$

from which it follows that the mean number of sides per grain, $\langle s \rangle$, is

$$\langle s \rangle = 2(e/c) = 6[1 - (2c'/3c)]$$
$$\sim 5.97 \qquad \ldots\ldots\ldots\ldots (21)$$

for a Johnson-Mehl microstructure in which $\sim$0.7% of the grains are caps.

If the caps are simply ignored, on the grounds that they are infrequent and are very likely to be etched out during metallographic preparation of microstructural sections of any real material having the Johnson-Mehl microstructure, then equations (16) and (17) apply and the mean number of sides per grain is 6.

The distribution of sidedness for grain sections through the Johnson-Mehl microstructure is given in figure 7(b). This distribution ignores the occurrence of caps, but is negligibly perturbed if the caps are included. It was obtained by analyzing 4200 grain sections. The distribution has a slightly wider spread than the corresponding distribution for the cellular microstructure. This broadening is largely due to the presence of a significant population of two-sided grain sections (lens-shaped figures apparent in figure 3a), whose occurrence is forbidden in the cellular microstructure. The mean of this distribution is 6; the standard deviation is 2.16.

(2) Cross-sectional area

The expected value of the area of a planar section through a grain of the cellular microstructure was computed by Meijering[5]. Using the result, by Smith and Guttman[12], that

$$P_A = 1/2\ (L_V), \qquad \ldots\ldots\ldots\ldots\ldots (22)$$

where P_A is the number of nodal points at which three grain sections meet per unit area of a planar section and L_V is the cell edge length per unit volume, it follows from equations (16) and (17) and from the Meijering value for the expected edge length per cell (Table I) that

$$N_A = 1.458b^{-2}, \qquad \ldots\ldots\ldots\ldots (23)$$

where N_A is the number of cells per unit area of a random planar section. The expected area per grain is then

$$\langle A \rangle = 1/N_A = 0.686b^2. \qquad \ldots\ldots\ldots\ldots (24)$$

Computer analysis of planar sections of the cellular microstructure containing an aggregate of 5400 grains gave the result

$$\langle N_A \rangle = 1.451b^{-2} \qquad \ldots\ldots\ldots\ldots (25)$$

in excellent agreement with the theoretical prediction.

The corresponding analysis of the Johnson-Mehl microstructure is again complicated by the presence of grain caps in two-dimensional sections; the available theory does not permit an exact calculation. The number $(N_A - N_A')$ of "normal" grain cross-sections per unit area may, however, be found. Using equations (19) and (20), and the appropriate modification of equation (22), we obtain

$$\begin{aligned}(N_A - N_A') &= 1/2\ (P_A - N_A') \\ &= 1/4\ L_V. \end{aligned} \qquad \ldots\ldots\ldots\ldots (26)$$

The theoretical calculations[5] for the mean grain boundary trace

length per cell in the Johnson-Mehl microstructure then gives

$$(N_A - N_A') = 1.140\ (\dot{N}/G)^{1/2}$$
$$= 1.225\ b^2. \qquad \ldots\ldots\ldots\ldots\ (27)$$

Computer analysis of sections of the Johnson-Mehl microstructure containing a total of 2532 grains yielded the experimental result

$$\langle N_A - N_A' \rangle^{EXP}_{JM} = 1.217\ b^2, \qquad \ldots\ldots\ldots\ldots\ (28)$$

in agreement with theory.

Computer analysis found 18 grain caps among 2532 grain sections of the Johnson-Mehl microstructure, giving a frequency of appearance of

$$(N_A' / N_A) \cong 0.0071\ . \qquad \ldots\ldots\ldots\ldots\ (29)$$

It then follows from equation (22) that

$$N_{A,JM} \cong 1.148\ (\dot{N}/G)^{1/2}$$
$$= 1.238\ b^2 \qquad \ldots\ldots\ldots\ldots\ (30)$$

and that

$$\langle A \rangle_{JM} = (N_{A,JM})^{-1} \cong 0.871\ (\dot{N}/G)^{-1/2}$$
$$= 0.807\ b^2, \qquad \ldots\ldots\ldots\ldots\ (31)$$

very close to the Meijering limit

$$\langle A \rangle_{JM} < 0.816\ b^2\ . \qquad \ldots\ldots\ldots\ldots\ (32)$$

The computer-generated distributions of grain section sizes in the cellular and Johnson-Mehl microstructures are given in figures 8 and 9. Figure 8 shows the functions $\rho(A/\langle A \rangle)$; figure 9 gives the functions $\rho(D/\langle D \rangle)$, where $D = \sqrt{A}$, the form in which grain size data is sometimes discussed and plotted. The normalized standard deviations of $\rho(A/\langle A \rangle)$ are 0.43 for the cellular microstructure and 0.51 for the Johnson-Mehl microstructure.

The grain size distributions do reveal qualitative differences

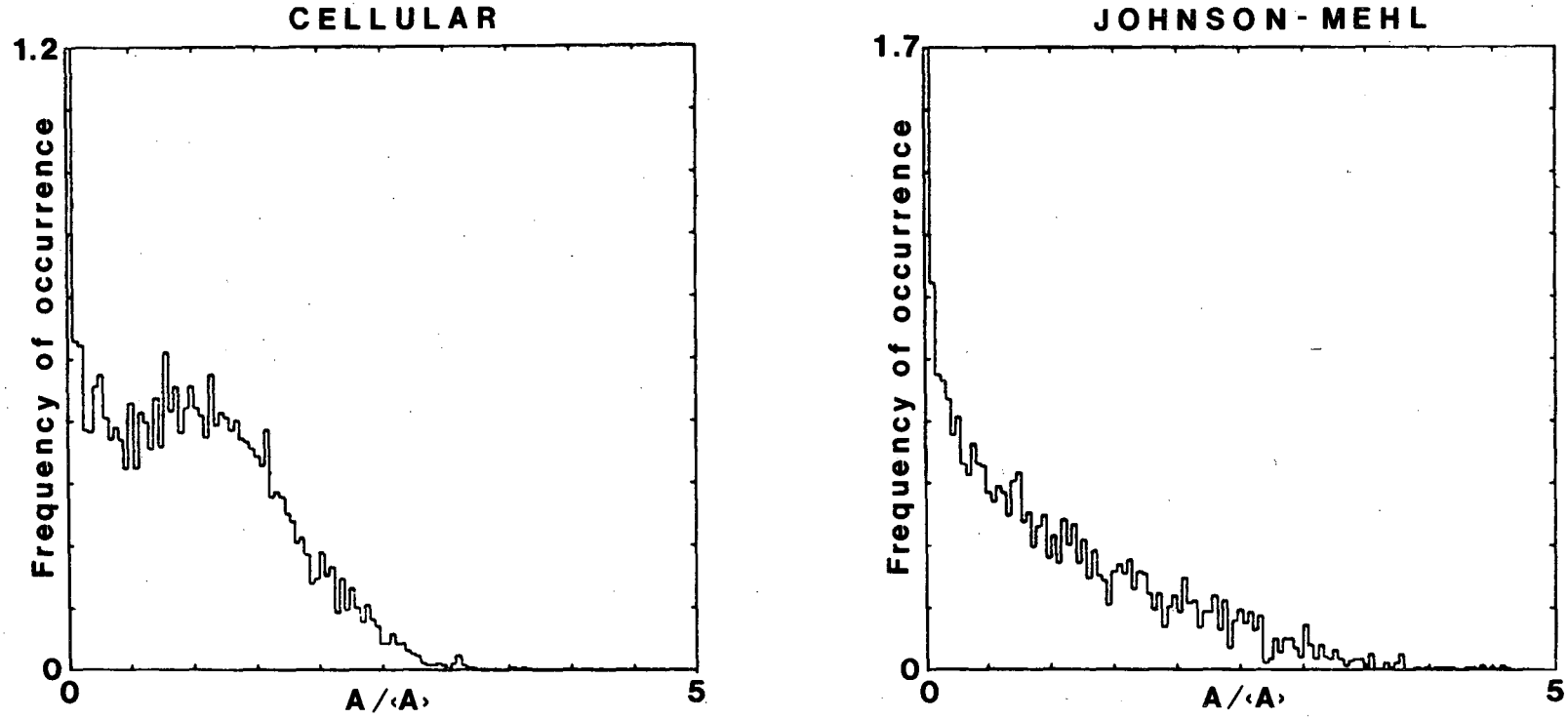

Figure 8. The distribution of grain section areas (A/⟨A⟩) for planar sections through the (a) Cellular and (b) Johnson-Mehl microstructures.

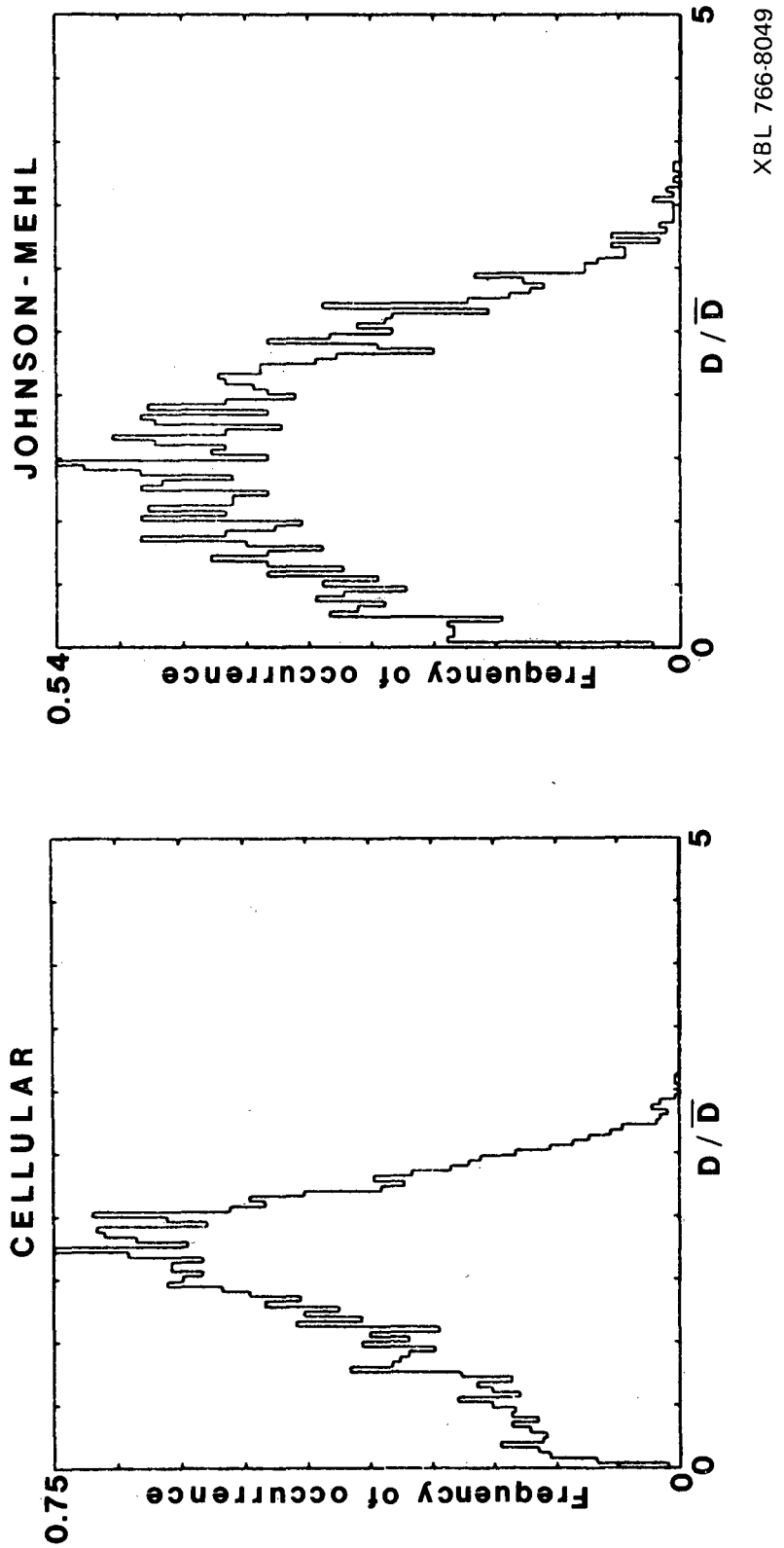

Figure 9. The distribution of effective grain diameter ($D/\langle D\rangle$; $D = A^{-\frac{1}{2}}$) for sections through the (a) Cellular and (b) Johnson-Mehl microstructures.

between the two microstructures. The most immediately evident of these is the subsidiary maximum in the distribution of $\rho(A/\langle A\rangle)$ for the cellular case, at $A/\langle A\rangle \sim 1$, which does not appear in the Johnson-Mehl distribution. This secondary maximum reflects the greater uniformity of grain size in the cellular microstructure, expected from the manner in which the microstructure is formed. The relative sharpness of the grain size distribution for the cellular microstructure is also apparent in the plots of $\rho(D/\langle D\rangle)$. It should, of course, be recognized that the distribution of $(D/\langle D\rangle)$ may be derived from the distribution of $(A/\langle A\rangle)$ and contains no new information.

(3) Intercept length

The mean value of the intercept length, or distance between successive grain boundary traces intersected with a randomly scribed line (Fig. 6) can be calculated exactly for both microstructures. As Smith and Guttman[12] have shown

$$\langle \ell \rangle = 2/S_V \, , \qquad \ldots\ldots\ldots\ldots\ldots \quad (33)$$

where S_V is the grain surface area per unit volume. It follows from equation (33) and from the data given in Table I, that

$$\langle \ell \rangle_{cell} = 0.687\ b \, , \qquad \ldots\ldots\ldots\ldots\ldots \quad (34)$$

while

$$\langle \ell \rangle_{JM} = 0.778\ b. \qquad \ldots\ldots\ldots\ldots\ldots \quad (35)$$

The larger value of the mean intercept length in the Johnson-Mehl microstructure appears to reflect the more equiaxed character of the grains in this microstructure, as seen qualitatively in figure 3b.

Computer analysis of 1241 test line intercepts obtained from the cellular microstructure yielded an average segment length of 0.674b, while measurement of 982 intercept lengths through the Johnson-Mehl microstructure gave an average length of 0.744b, both in reasonable agreement with the theoretical prediction.

The segment length distributions, $\rho(\ell/\langle\ell\rangle)$, are plotted for the two microstructures in figure 10. While the two histograms are not identical, they are very similar. In particular, the qualitative difference evident in the areal distributions is not present. The standard deviations are $\sim 0.57\langle\ell\rangle$ and $\sim 0.63\langle\ell\rangle$ for the cellular and Johnson-Mehl microstructures, respectively. The similarity in the deviations further documents the similarity between the distributions.

IV. Discussion

A. Microstructural Characteristics

The complexity of the histograms of microstructural features is a consequence of the fact that each is a product of two statistical processes: the inherent irregularity in the grain size and shape within the microstructure, and the induced irregularity due to the bias introduced by the intersection of a random plane with the grains to produce a two-dimensional section. Available theoretical analyses do not permit a clear separation of the two effects in the absence of a full three-dimensional characterization of the microstructure.

The most obvious and interesting feature of the geometric distributions is the clear qualitative difference between the areal distributions in the Johnson-Mehl and cellular microstructures,

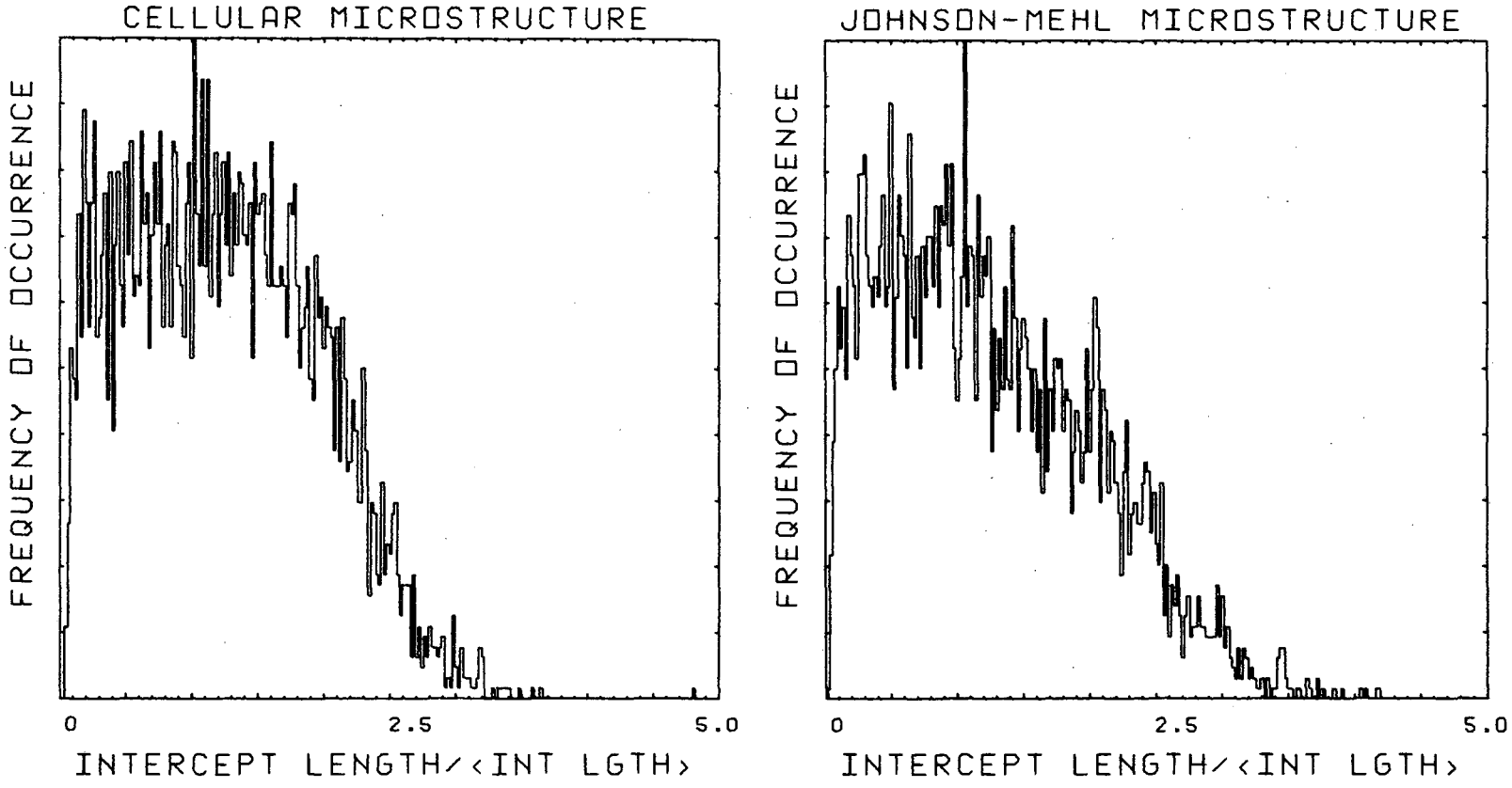

Figure 10. The distribution of intercept lengths for sections through the (a) Cellular and (b) Johnson-Mehl microstructures.

coupled with the fact that this distinction is not observed in the intercept length distributions.

These features of the distributions are consistent with an expected tendency for the grains of the cellular microstructure to be more nearly uniform in volume, but less nearly equiaxed, than the grains of the Johnson-Mehl microstructure. The more uniform volume distribution of the cellular grains is anticipated since these grains will be unusually small (large) only if they occur in a region which is restricted (expanded) by the presence (absence) of other nearby nuclei. Grains of the Johnson-Mehl microstructure will be unusually small either if they are restricted by adjacent nuclei or if they form very late in the transformation processs. The more angular appearance of the cellular grains (which was inferred by Meijering[5] and is apparent in the microstructure shown in figure 3a) is expected since the nuclei surrounding a growing grain are randomly distributed and unlikely to be symmetrically disposed. In the Johnson-Mehl process, on the other hand, the spherical growth of a grain inhibits (by prior transformation) the formation of immediately adjacent nuclei and promotes nucleation in spherical shells after some growth has taken place.

While the distribution of grain section sizes is insensitive to the shape of the grain sections, the distribution of intercept lengths is very sensitive to grain shape; elongated grains lead to a high density of relatively short segments. The combination of grain size and grain shape leads to the similarity of the intercept length distributions for the two microstructures.

B. Experimental evidence for the Johnson-Mehl microstructure

While there are a number of metals, for example, bronze and some stainless steels, which are often found to have microstructures with the straight grain boundaries characteristic of a cellular process, there do not appear to be published microstructural analyses which can be compared to the theory. On the other hand, examples of microstructures resembling the Johnson-Mehl microstructure are known.

The classic example of a Johnson-Mehl microstructure type is recrystallized Armco iron, which was studied in detail by Schiel and Wurst[13] some years before the Johnson-Mehl process was described theoretically. In their original treatment, Johnson and Mehl[1] obtained an approximate form for the distribution of grain diameters in the microstructure and found reasonable agreement with the Schiel-Wurst data. The agreement is made even better if the more precise computer-generated histogram is used, as shown in figure 11. Meijering[5] estimated the mean section size in the microstructure by graphically integrating the Schiel-Wurst data. His result,

$$\langle A \rangle = 0.80\ b^2 \qquad \ldots\ldots\ldots\ldots\ldots\ldots \quad (36)$$

was in good agreement with his estimate ($\langle A \rangle$ $\langle 0.816b^2$), and is in even better agreement with the computer result $\langle A \rangle = 0.807b^2$.

The Johnson-Mehl microstructure may be common in recrystallized iron, as further evidenced by the microstructure of a sample of commercial Fe-Si, of uncertain processing history, available in our laboratory. Its microstructure is compared to the computer-generated Johnson-Mehl microstructure in figure 12. The qualitative similarity

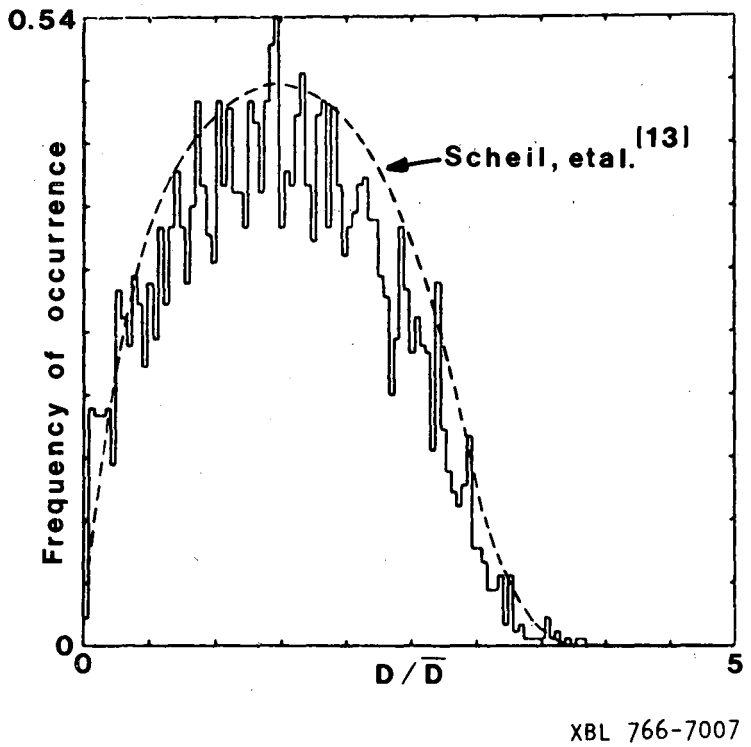

Figure 11. The distribution of grain diameters measured by Schiel and Wurst[13] for recrystallized Armco iron compared to the Johnson-Mehl distribution.

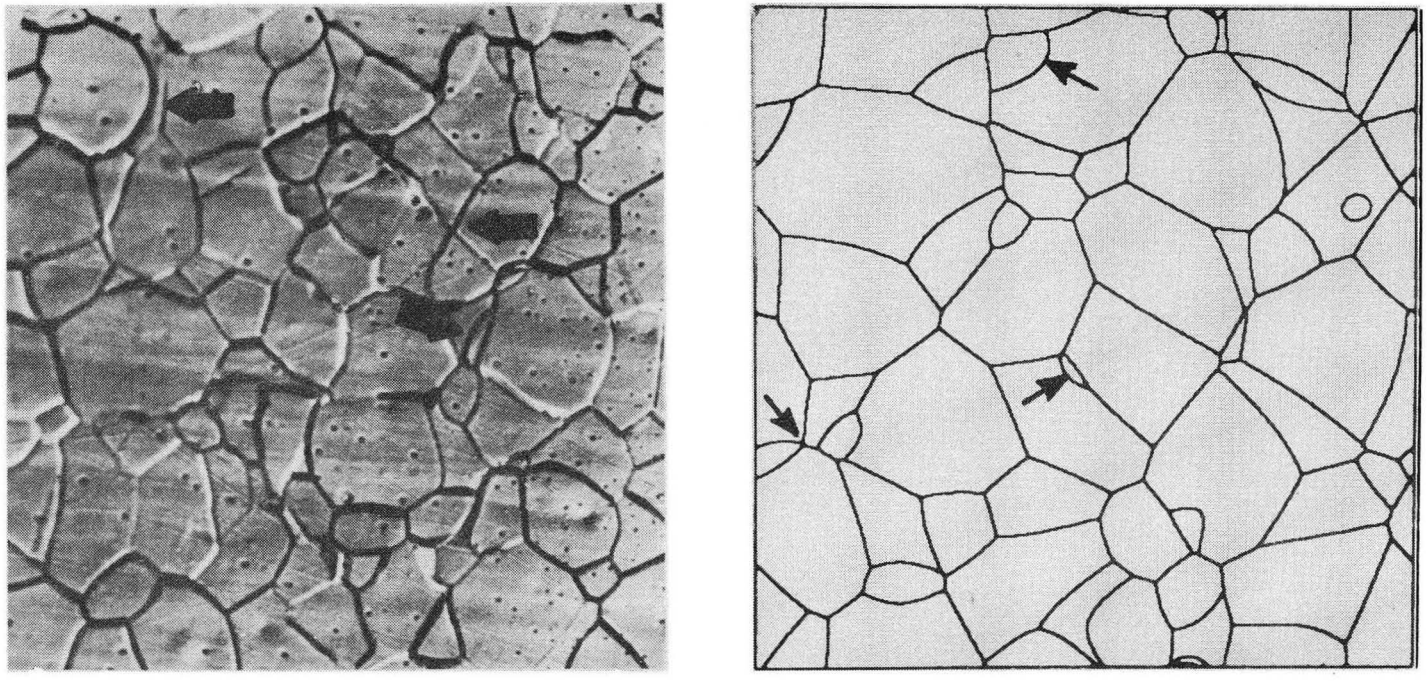

XBB 792-2552

Figure 12. (a) The microstructure of a sample of commercial recrystallized Fe-Si.

(b) The computer-generated Johnson-Mehl microstructure. The arrows in the figures indicate comparable features. The apparent "four-grain" junction in the Johnson-Mehl microstructure is actually two three-grain junctions separated by a short grain boundary.

is evident. The distribution of grain section areas is plotted in figure 13 in comparison with the corresponding distribution for the Johnson-Mehl microstructure. The quantitative agreement is also good.

A rather different (and initially surprising) example of the Johnson-Mehl process was found by Van der Biest and Thomas[14] in their in situ studies of the ordering reaction in lithium ferrite within a transmission electron microscope equipped with an environmental stage. By direct measurement of nucleation and growth rates, they determined that the reaction is well-approximated by the Johnson-Mehl process. The similarity is illustrated in figure 14, in which we compare a transformation sequence of micrographs taken by Van der Biest and Thomas[14] with a similar sequence developed in the computer using the experimentally measured nucleation and growth rates. The correspondence between the two cases is still more evident when computer generated motion pictures are compared to the real time movie generated in the microscope.

IV. Conclusion

The Johnson-Mehl and cellular microstructure types arise naturally from the classical model of a phase transformation in a one-component solid through growth from a random distribution of nucleation sites. The Johnson-Mehl microstructure results in the kinetic limit of a constant nucleation rate over an essentially constant density of available nucleation sites; the cellular microstructure is produced in the kinetic limit of simultaneous activation of the available nucleation sites. Members of each of these microstructure types

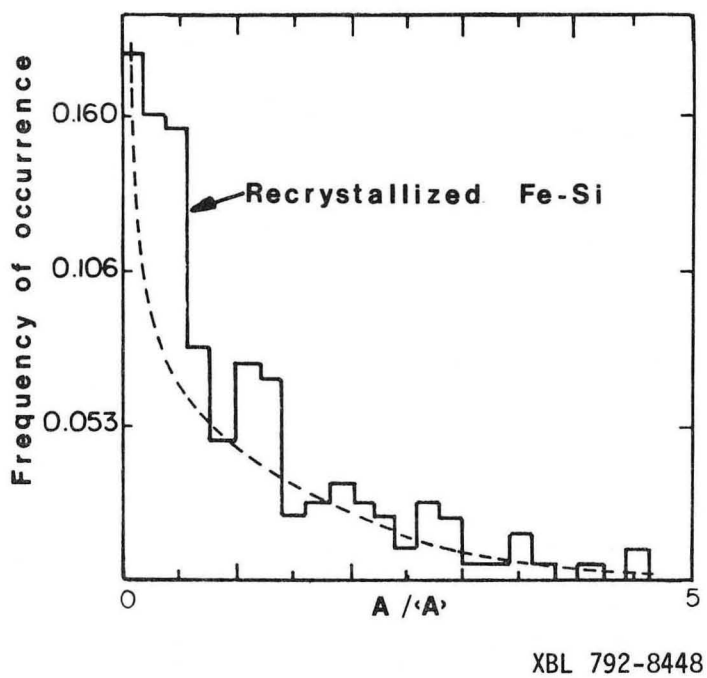

Figure 13. Histogram of grain areas for the microstructure shown in Figure 12, compared to the Johnson-Mehl distribution (dotted line).

GROWTH SEQUENCE FOR ORDERING IN $LiFe_5O_8$
COMPARED WITH A COMPUTER SIMULATED GROWTH SEQUENCE

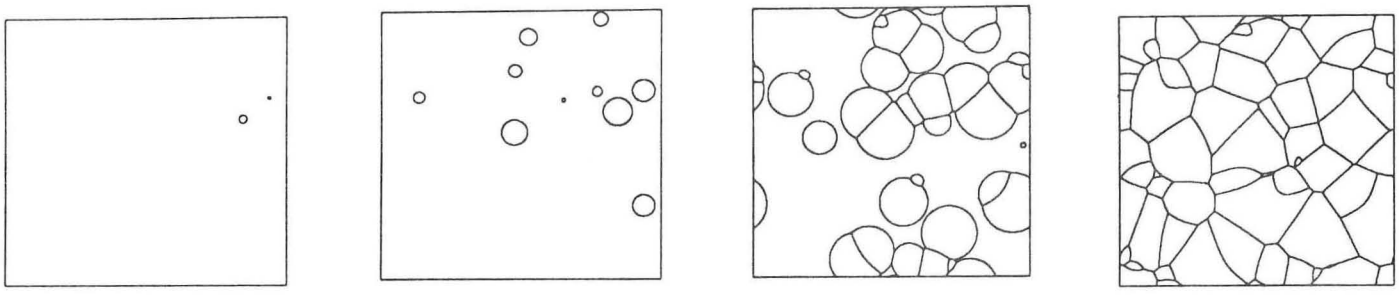

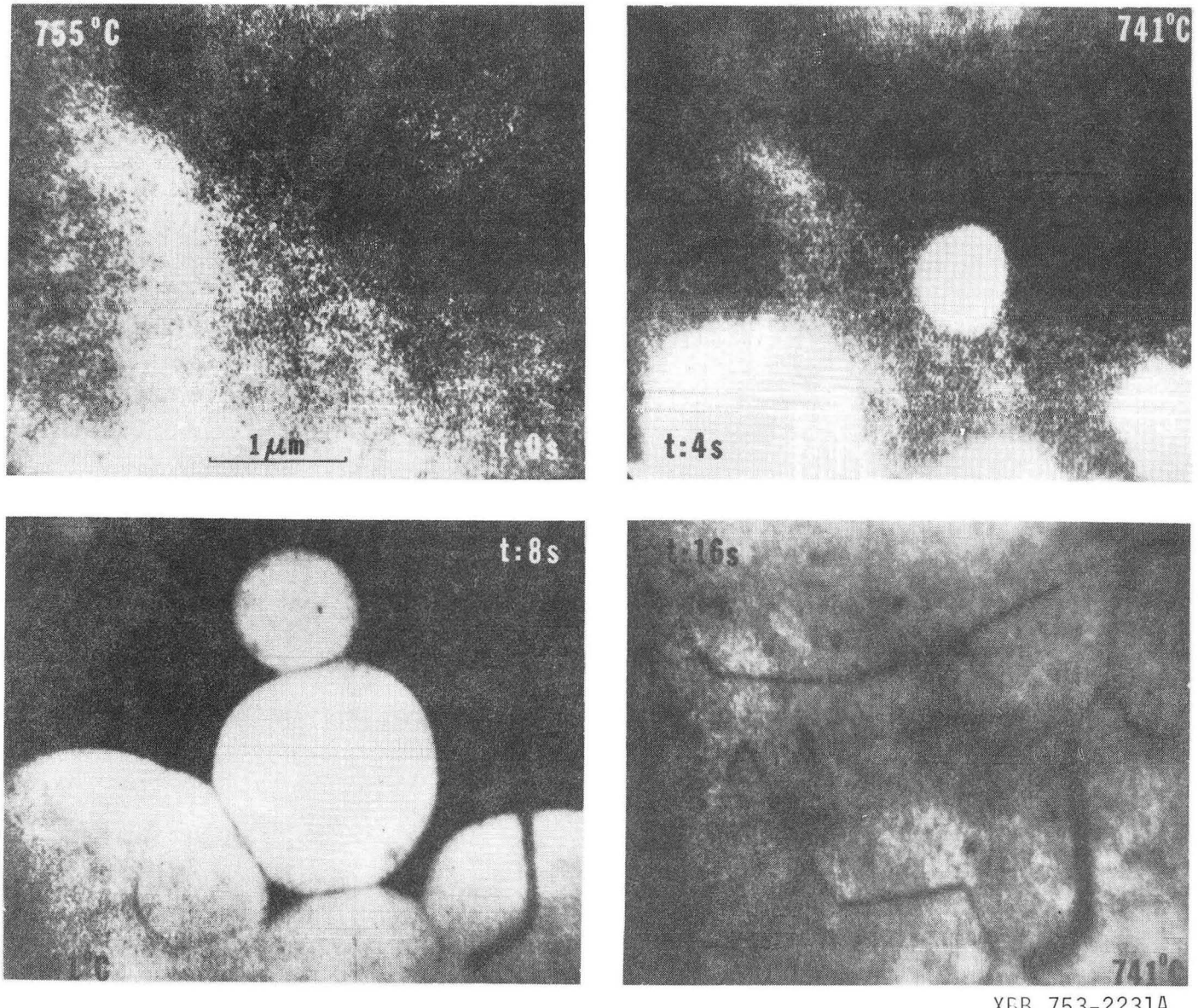

XBB 753-2231A

Figure 14. Time lapse sequence of the ordering transformation in lithium ferrite, made by Van Der Biest and Thomas[14] in a transmission electron microstructure, compared to a computer-generated sequence for the Johnson-Mehl process.

are similar to one another in all aspects of their geometrical statistics; they differ only through a homogeneous expansion or contraction. Their geometric features can be, and in many respects have been, characterized through a combination of analytic and computer simulation studies. Comparison with available experimental results shows that the Johnson-Mehl microstructure compares well with such metallurgically diverse experimental structures as the recrystallization structure of silicon iron and the intermediate structures established during the ordering of lithium ferrite. These correspondencies suggest that the idealized microstructures studied here may be physically relevant as well as being pedagogically useful.

Acknowledgement

This work was supported by the Division of Materials Sciences, Office of Basic Energy Sciences, U. S. Department of Energy under Contract No. W-7405-Eng-48.

References

1. W. A. Johnson and R. F. Mehl, Trans. AIMME, 135, 416 (1939).

2. M. Avrami, J. Chem. Phys., 7, 1103 (1939); 8, 212 (1940); 9, 177 (1941).

3. J. W. Cahn, Acta Met., 4, 449 (1956).

4. J. W. Christian, The Theory of Transformations in Metals and Alloys,1st edition, Pergamon Press, Oxford, (1965), Chapt. XII.

5. J. L. Meijering, Phillips Res. Repts., 8, 270 (1953).

6. K. W. Mahin, M. S. Thesis, Dept. Materials Science and Engineering, University of California, Berkeley (1976).

7. K. W. Mahin, K. Hanson, and J. W. Morris, Jr., in Computer Simulation for Materials Applications, R. Arsenault, J. Simmons and J. Beeler, eds., National Bureau of Standards, Gaithersburg, (1976), p. 31.

8. W. Feller, An Introduction to Probability Theory and its Applications, J. Wiley New York (1950), Vol. I.

9. K. Hanson, Acta Met. (in press).

10. U. R. Evans, Trans. Faraday Soc., 41, 365 (1945).

11. C. S. Smith, in Metal Interfaces, Am. Soc. Metals, Cleveland, (1951), p. 65.

12. C. S. Smith and L. Guttman, J. Metals, 5, 8, (1955).

13. E. Schiel and H. Wurst, Z. Metal., 28, 340 (1936).

14. O. Van der Biest and G. Thomas, in Electron Microscopy In Mineralogy, H. R. Wenk, Ed., Scrinoer, Berlin, (1976), p. 280.

Figure Captions

Figure 1. Time-lapse sequence showing development of the cellular microstructure as seen on a planar section through the transforming body.

Figure 2. Time-lapse sequence showing development of the Johnson-Mehl microstructure as seen on a planar section through the transforming body.

Figure 3. Examples of sections through (a) the Cellular and (b) the Johnson-Mehl microstructure.

Figure 4. The surface of impingement between two grains in the Johnson-Mehl microstructure.

Figure 5. A serial section through the Johnson-Mehl microstructure. The second and third frames contain grain "caps".

Figure 6. A planar section of the microstructure intersected randomly by a lineal grid, yielding a number of intercept lengths, ℓ_1, ℓ_2, etc.

Figure 7. The distribution of the number of sides per grain for the (a) Cellular and (b) Johnson-Mehl microstructures.

Figure 8. The distribution of grain section areas ($A/\langle A\rangle$) for planar sections through the (a) Cellular and (b) Johnson-Mehl microstructures.

Figure 9. The distribution of effective grain diameter ($D/\langle D\rangle$; $D = A^{-\frac{1}{2}}$) for sections through the (a) Cellular and (b) Johnson-Mehl microstructures.

Figure 10. The distribution of intercept lengths for sections through the (a) Cellular and (b) Johnson-Mehl microstructures.

Figure 11. The distribution of grain diameters measured by Schiel and Wurst[13] for recrystallized Armco iron compared to the Johnson-Mehl distribution.

Figure 12. (a) The microstructure of a sample of commercial recrystallized Fe-Si.

(b) The computer-generated Johnson-Mehl microstructure. The arrows in the figures indicate comparable features. The apparent "four-grain" junction in the Johnson-Mehl microstructure is actually two three-grain junctions separated by a short grain boundary.

Figure 13. Histogram of grain areas for the microstructure shown in Figure 12, compared to the Johnson-Mehl distribution (dotted line).

Figure 14. Time lapse sequence of the ordering transformation in lithium ferrite, made by Van Der Biest and Thomas[14] in a transmission electron microstructure, compared to a computer-generated sequence for the Johnson-Mehl process.

TECHNICAL INFORMATION DEPARTMENT
LAWRENCE BERKELEY LABORATORY
UNIVERSITY OF CALIFORNIA
BERKELEY, CALIFORNIA 94720